

NUMERICAL SIMULATION OF TURBULENT FLOW IN VENTILATION DUCTS

N Jovicic¹, D Milovanovic¹, M Babic¹ and J V Soulis²

¹ University of Kragujevac, Faculty of Mechanical Engineering
Sestre Janjic 6, 34 000, Kragujevac, Yugoslavia

² Democriton University of Thrace, Department of Civil Engineering,
Hydraulics Division, Xanthi, Greece

ABSTRACT

An efficient numerical method for solving the Reynolds-Averaged Navier-Stokes (RANS) equations with turbulence models for complex geometry and high Reynolds number flows is used to perform a highly-resolved computation of the turbulent flow in a strongly curved part of a ventilation duct.

The three-dimensional incompressible RANS equations and the isotropic $k-\omega$ two-equation near-wall turbulence closure are written in generalized curvilinear coordinates in the strong conservation form. The discrete mean flow and turbulence closure equations are advanced in time using pointwise implicit four-stage Runge-Kutta scheme enhanced with local time stepping, variable coefficients implicit residual smoothing and multigrid acceleration.

The turbulent flow through a strongly curved bend features pressure-induced secondary motions and rotation effects on turbulence. The Reynolds number based on the bulk axial velocity was 56690. The general conclusion is that the RANS equations in conjunction with the isotropic two-equation near-wall model describes most global features of the flow, but needs some further improvement to resolve some subtle details that are not fully captured by the method.

Keywords: CFD, Duct, Modeling, Ventilation

INTRODUCTION

Advances in computing resources are playing important role in the recent trend of increased use of Computational Fluid Dynamics (CFD) to predict practical engineering problems by solving Navier-Stokes equations with high resolution schemes. Flows in ducts with curvature experience pressure- and turbulence-induced secondary motions. These are of academic interest but also have very significant consequences in many industrial applications involving heat and mass transfer. Incompressible turbulent flow in a U-bend is probably the one of the most challenging problems in CFD. Numerical simulation of high Reynolds number turbulent flows in 180 degree bends requires a very large number of grid points and extremely small grid spacing in order to resolve phenomena in near-wall region. Such meshes can dramatically deteriorate the convergence rate of numerical procedure. In order to make accurate, efficient and low-cost codes for engineering purposes it is very desirable to apply modern acceleration techniques. Among these, the multigrid method is one of the most efficient and general techniques [1]. The advantage of the multigrid method over other acceleration techniques is the fact that the rate of convergence is independent of the size of the system to be solved. It is especially useful for the simulation of three-dimensional turbulent flow in complex domains

that have to be discretized by highly stretched, large aspect-ratio computational meshes. With much success, the multigrid method has been applied in CFD applications involving both compressible [2] and incompressible flows [3], [4], [5]. The multistage Runge-Kutta scheme, developed by Jameson [6], in conjunction with local time stepping, implicit residual smoothing and the multigrid method is a powerful tool for solving real-life internal flow problems.

In this paper, we present the results of an incompressible multigrid three-dimensional Navier-Stokes code for the analysis of internal flows. We describe its application to the computation of incompressible turbulent flow through a 180 degree bend with a square cross-section, for which Choi [7] have provided detailed experimental data. The flow through a curved duct has previously been calculated by Chang [8] and Choi [9] using a numerical solution of the RANS equation. Chang [8], used the $k-\varepsilon$ turbulence model and a relatively coarse grid, which caused significant deviations between measured and computed results, especially for bend angles larger than 45° . Choi [9] performed finer-grid computations using an algebraic second-moment closure (ASM) and obtained a generally satisfactory description of the Reynolds stress field. However, even with the most refined grid some discrepancies between the experiment and computed development are apparent. We present a method, which uses a two-equation near-wall turbulence model that allows us to set more grid points near the passage walls, giving closer agreement with computations.

NUMERICAL METHOD

The three-dimensional incompressible RANS equations with isotropic two-equation, near-wall turbulence closures, are written in generalized curvilinear coordinates in strong conservation form [10]. The $k-\omega$ model [11] is chosen because it is the only available closure without restrictions on the distance from the wall to the near-wall grid point, which is very appropriate for complex geometrical configurations.

The artificial compressibility method is employed to couple the velocity and pressure field in the mean flow equations. The governing equations are discretized on a collocated mesh using the cell vertex finite volume method. The convective fluxes are discretized using second-order central-differencing in conjunction with flux difference splitting upwind third-order accuracy scheme [12]. Three-point central differencing is employed for the viscous fluxes and source terms in turbulence closure equations. The discrete mean flow and turbulence closure equations are advanced in time using a pointwise implicit [13] four-stage Runge-Kutta scheme enhanced with local time stepping, variable coefficients implicit residual smoothing and multigrid acceleration. For most two-equation models, the source terms are usually dominant and become stiff near the solid wall and the efficiency of solution then totally depends on the treatment of those source terms. In our numerical model, the source terms in the k and ω equations are divided into two groups locally according to their sign and then only negative parts are treated implicitly. That so-called point-implicit technique is employed to improve the efficiency of the solution and to alleviate the stiffness of the governing equations in the near-wall region. In the present paper the local time step limit is computed with scaled spectral radii of the flux Jacobian matrices for the convective terms. A variable coefficients implicit residual smoothing is used to extend the stability limit and robustness of the basic scheme. The variable coefficients depend on the spectral radii of the flux Jacobian matrices as well as Courant numbers of the smoothed and unsmoothed scheme. A time-lagged or loosely-coupled approach is employed in solving the Navier-Stokes equations and two equation turbulence model in a time marching method, i.e., mean flow and turbulence closure equations are solved separately. A three level V-cycle multigrid algorithm with semi-coarsening in the transverse plane is applied only to the mean flow equations with one, two

and three iterations performed on the first, second and third grid level, respectively. The turbulence closure equations are solved only on the finest mesh and eddy viscosity is injected to the coarser meshes and kept frozen during the multigrid process. Three single-grid iterations are performed on the turbulence closure equations per multigrid cycle [3].

APPLICATIONS

Choi et al. (1990) provided detailed experimental data of the development of air turbulent flow with constant temperature through a 180 deg square-sectioned bend. The duct geometry is shown in Fig. 1. The bend section was connected to straight inlet and outlet tangents, all of square section $D \times D = 88.9 \times 88.9$ mm. Centerline curvature radius of the bend was $R_c = 3.357D$.

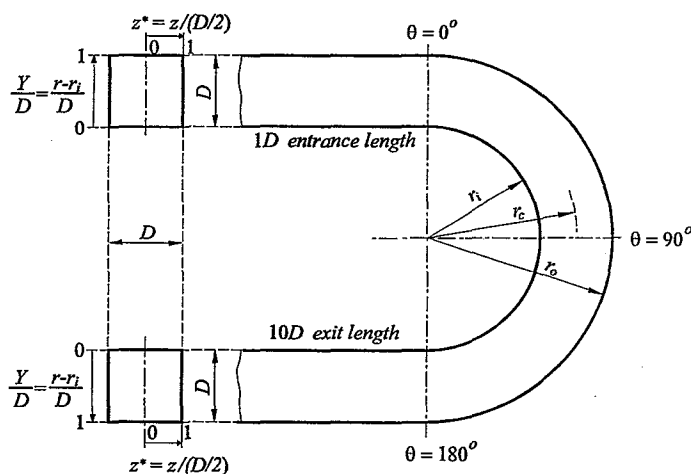


Fig. 1 Flow geometry and coordinate system used

The inlet bulk axial velocity was 11m/s, which corresponds to a fully developed turbulent flow in a square section duct. The Reynolds number based on the bulk axial velocity and hydraulic diameter was 56690. Due to symmetry of the flow field, one half of domain is considered, with $Z=0$ as a plane of symmetry. Domain is discretized by 200000 grid points (streamwise x radial x normal = 93 x 65 x 33).

Measurements of velocity components within a cross-section located one hydraulic diameter upstream of the bend are available as inflow conditions. Values for turbulent kinetic energy and specific dissipation rate at inlet are obtained from a previous numerical simulation of a 100D long straight duct flow.

Numerical results of the mean flow at a distance of one hydraulic diameter upstream show that the flow is slightly influenced by the bend. Namely, the favorable streamwise pressure gradient along the inner wall of the bend induces a mean transverse flow directed along the inner wall, which is noticeable at a small distance upstream. This effect was taken into account by starting the computations one hydraulic diameter upstream with a flow pattern corresponding to the fully developed turbulent duct flow.

The computed velocity components for three streamwise stations (at 45° , 90° and 135°) are plotted in Fig. 4-6. As far as the region between 0° and 45° is concerned, the influence of the bend is still relatively weak. The profiles of streamwise velocity component (Fig. 2) show their maximum values displaced towards the inner radius wall, due to the favorable streamwise pressure gradient there. Also, the radial velocity component is mostly directed to the inner wall (Fig. 3). The flow pattern in this region indicates the inception of the secondary flow influenced by transverse pressure gradients, which arise due to lateral curvature of the

main flow in the bend. The secondary flow is much more intense after 45° . There, the radial velocity component near the side wall ($z^*=0.75$) shows a negative values, while the profiles at other z locations are positive (Fig. 4) that is in close agreement with the experiment.

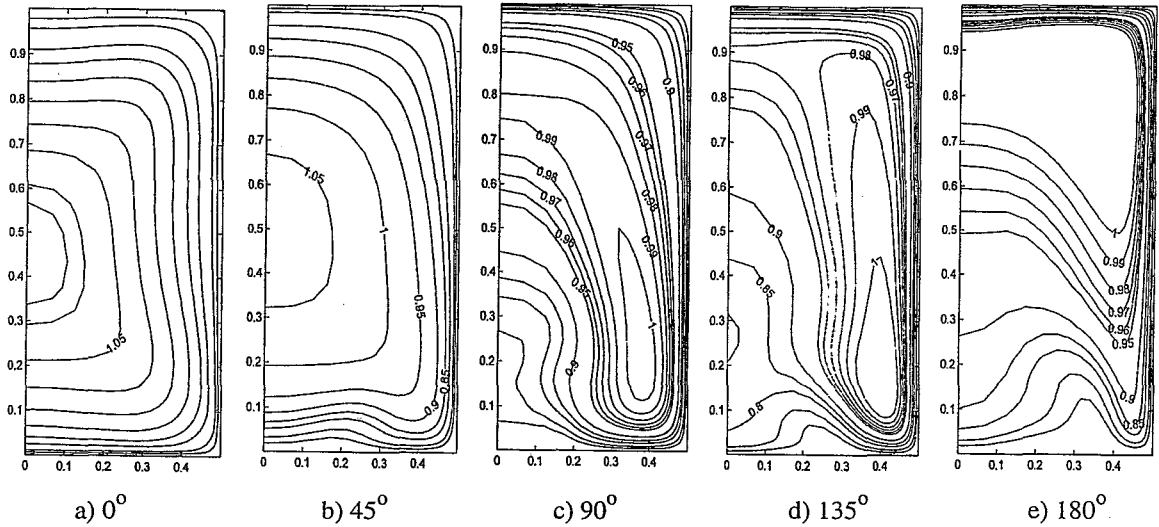


Fig. 2 Axial velocity contours at different bend sections

Figure 5 shows a local maximum of the streamwise velocity component near the inner wall at 90° in the plane of symmetry. The computational results are slightly different from the measured ones. A similar tendency was reported in [9]. In the region between 90° and 135° there is streamwise deceleration of the streamwise and radial velocity component due to the injection of low speed fluid from the peripheral region of the duct into the core of the flow. Further, towards to the exit of the bend, the maximum streamwise velocity is moved from inner to outer wall (Fig 2).

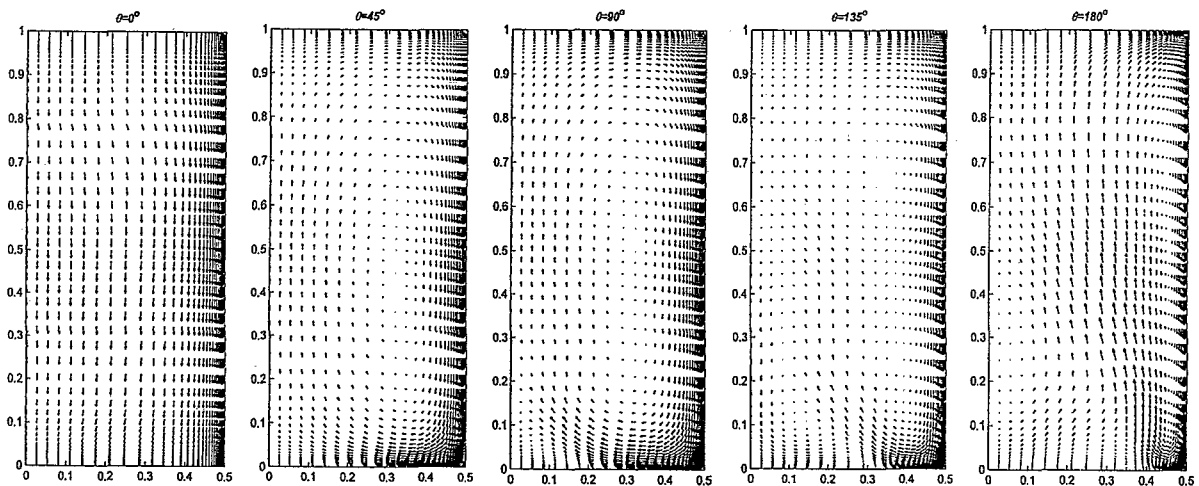


Fig. 3 Secondary flow vectors in the symmetry plane

Although there was no available experimental data for pressure in [7], the results for pressure distribution along the inner and outer wall are in close agreement with similar experiments presented in [8]. The maximum of the pressure is obtained at 45° on the outer wall, and the minimum value is found at the bend exit.

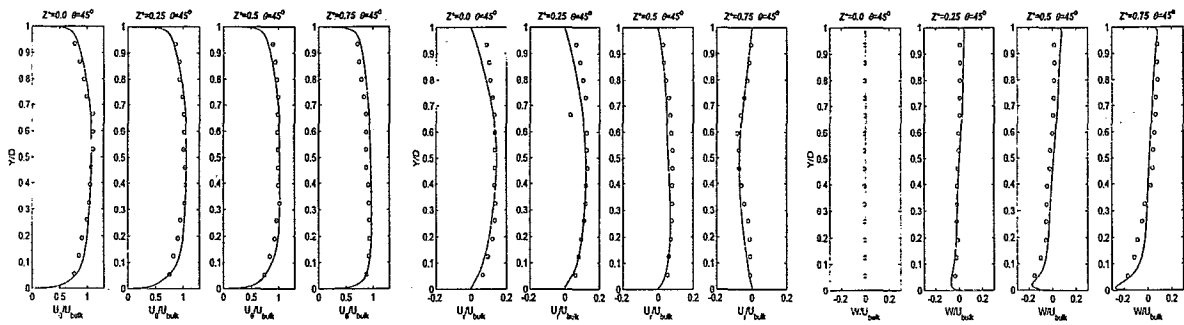


Fig. 4 Velocity component profiles at 45 deg.

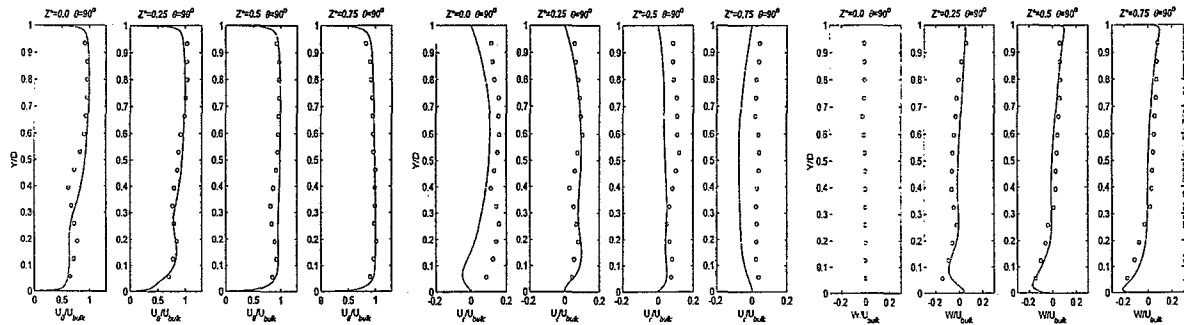


Fig. 5 Velocity component profiles at 90 deg.

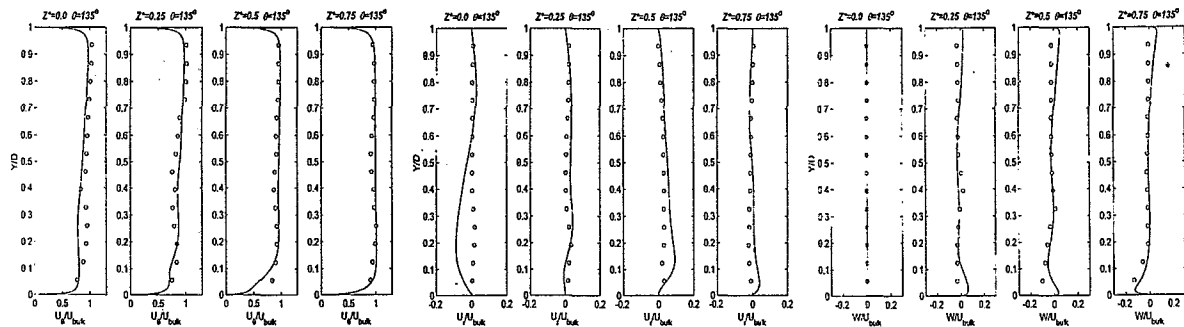


Fig. 6 Velocity component profiles at 135 deg.

CONCLUSION

A numerical model based on Reynolds Averaged Navier-Stokes equations with an isotropic two-equation near-wall turbulence model was used to simulate a complex three-dimensional flow field typical of ventilation systems. The results showed that most global features of the flow field are correctly resolved but noteworthy differences between measured and numerical results still remain. The same was found in [9], where the algebraic second-moment closure was employed. A key factor in obtaining the correct primary flow is the prediction of secondary motion with reasonable fidelity. The breakdown of the secondary motion into a complex multi-cellular pattern, at about 90 deg of the bend, leads to distortion of the streamwise velocity profile near the inner wall. Differences between measured and computed values at that location are probably due to failures of the isotropic two-equation turbulence model. The turbulence structures in a bend are significantly influenced by curvature of the bend, however, isotropic two-equations turbulence models fail in resolving that problem. Even with algebraic second-moment closure reported in [9] these differences exist, but in our

opinion this was due to relatively coarse grid used in their numerical calculation (47x25 in the transverse plane).

In order to predict secondary flow more precisely it is necessary to employ more grid points near the walls. Also, non-linear constitutive relations for Reynolds stress tensor components instead of Boussinesq's relation may lead to improved results.

REFERENCES

1. Hirsch, C. 1988. *Numerical Computation of Internal and External Flows*, Volume 2: Computational Methods for Inviscid and Viscous Flows, John Wiley & Sons.
2. Chima, R V, Yokota, J W. 1990. Numerical Analysis of Three-Dimensional Viscous Internal Flows, *AIAA Journal*, Vol. 28, No. 5, pp. 798-806.
3. Lin, F B, Sotiropoulos 1997. Strongly-Coupled Multigrid Method for 3-D Incompressible Flows Using Near-Wall Turbulence Closures, *Journal of Fluid Engineering*, Vol 119.
4. Sheng, C, Taylor, L, Whitfield D. 1994. A Multigrid Algorithm for Three-Dimensional Incompressible High Reynolds Number Turbulent Flows, *AIAA paper 94-2335*.
5. Emvin, P. 1997. The Full Multigrid Method Applied to Turbulent Flow in Ventilated Enclosures Using Structured and Unstructured Grids, *Ph.D. thesis*, Chalmers University of Technology, Sweden,
6. Jameson, A, Schmidt, W, Turkel, E. 1981. Numerical Solutions of the Euler Equations by Finite Volume Methods Using Runge-Kutta Time Stepping Schemes, *AIAA paper* No. 81 - 1259.
7. Choi, Y D, Moon, C, Yang, S H. Measurement of Turbulent Flow Characteristics of Square Duct with a 180 degree Bend by Hot Wire Anemometer, *International Symp. on Engineering Turbulence Modeling and Measurement, also ERCOFTAC Database*, Test 06, Fluidigo, University of Surrey, UK.
8. Chang, S M, Humphrey, J A C, Modavi, A. 1983. Turbulent Flow in a Strongly Curved U-bend and Downstream Tangent of Square Cross-Sections, *PHC Phys.Chem. Hydrodynamics*, Vol 4., No 3., pp. 243-269.
9. Choi, Y D, Iacovides, H, Launder, B E. 1989. Numerical Computations of Turbulent Flow in a Square Sectioned 180 deg Bend, *Journal of Fluids Engineering*, Vol. 111., pp. 59-68,
10. Soulis, J V, Jovicic, N, Milovanovic, D, et al 1998. Numerical Modeling of Incompressible Turbulent Flow in Turbomachinery, *Computational Fluid Dynamics '98* edited by Papailiou, K., et al., pp. 259-265, John Wiley&Sons.
11. Wilcox, D. 1994. Simulation of Transition with a Two-Equation Turbulence Model, *AIAA Journal*, Vol. 32, pp 247-255.
12. Rogers, S E, Kwak D. 1988. An Upwind Differencing Scheme for the Steady-State Incompressible Navier Stokes Equations, *NASA TM 101051*.
13. Zheng, S, Liao, C, Liu, C, Sung, C H, Huang, T T. 1997. Multigrid Computation of Incompressible Flows Using Two-Equations Turbulence Models: Part I - Numerical Method, *Journal of Fluids Engineering*, Vol. 119, pp. 893-899.